

## **Supplementary Information**

### **Rechargeable Na/Ni battery based on the Ni(OH)<sub>2</sub>/NiOOH redox couple with high energy density and good cycling performance**

Seungyoung Park,<sup>a</sup> Ziyauddin Khan,<sup>a</sup> Tae Joo Shin,<sup>b</sup> Youngsik Kim<sup>a</sup> and Hyunhyub Ko<sup>\*a</sup>

<sup>a</sup>School of Energy and Chemical Engineering, Ulsan National Institute of Science and Technology (UNIST), 50 UNIST-gil, Ulsan 44919, Republic of Korea

<sup>b</sup>UNIST Central Research Facilities (UCRF), Ulsan National Institute of Science and Technology (UNIST), 50 UNIST-gil, Ulsan 44919, Republic of Korea

\*Corresponding Author

Email: [hyunhko@unist.ac.kr](mailto:hyunhko@unist.ac.kr)

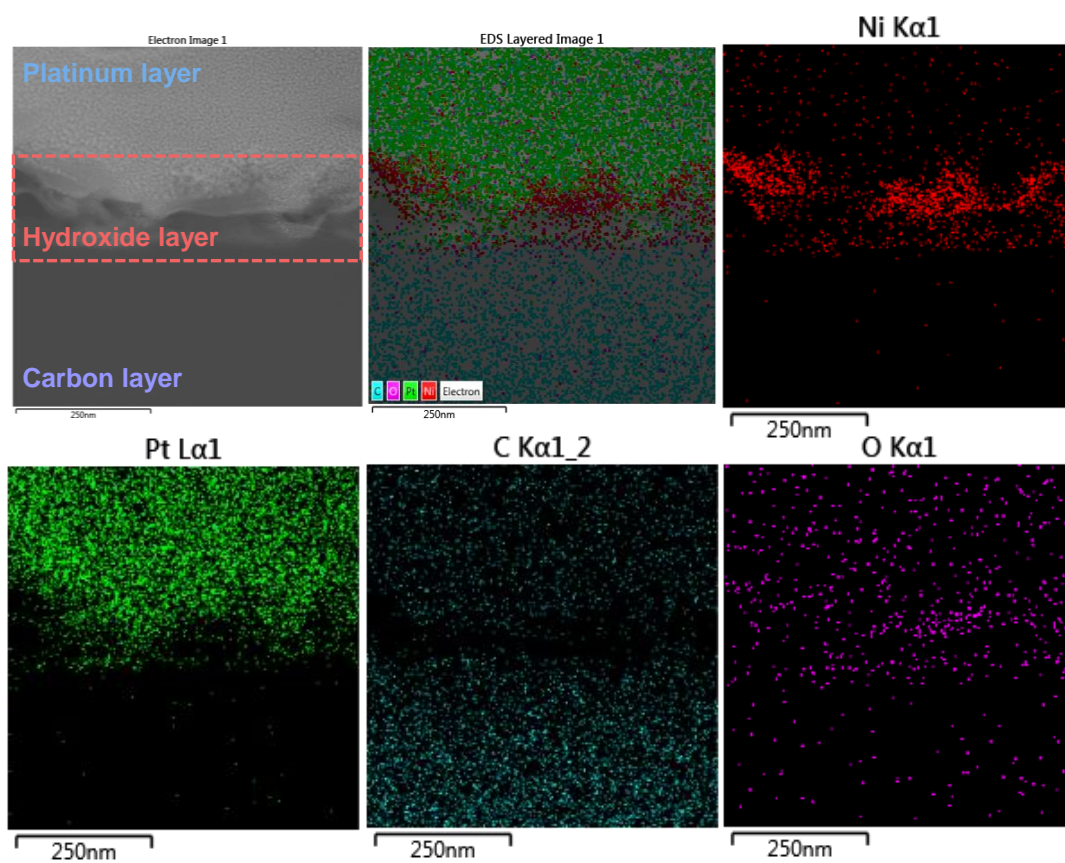


**Fig. S1** STEM-EDS cross-sectional mapping images of the hydroxide layer on the carbon microfiber electrode.

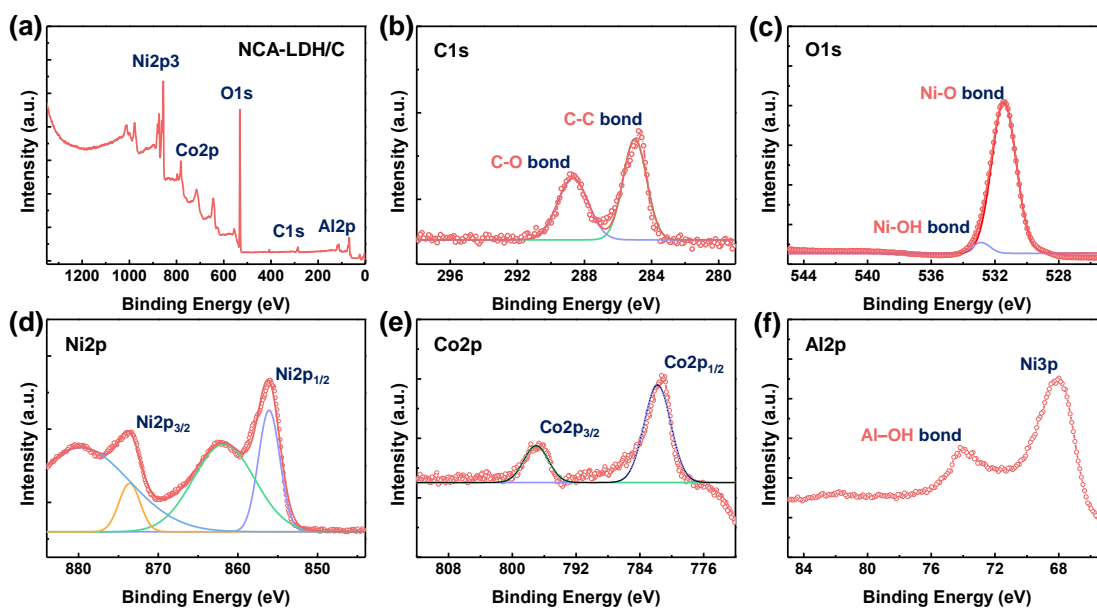


**Fig. S2** Summary of XPS spectra recorded to analyze the chemical bonding in the NCA-LDH/C electrode. (a) Summary XPS spectra, (b) C 1s spectrum, (c) O 1s spectrum, (d) Ni 2p spectrum, (e) Co 2p spectrum, and Al 2p spectrum of NCA-LDH/C electrode.

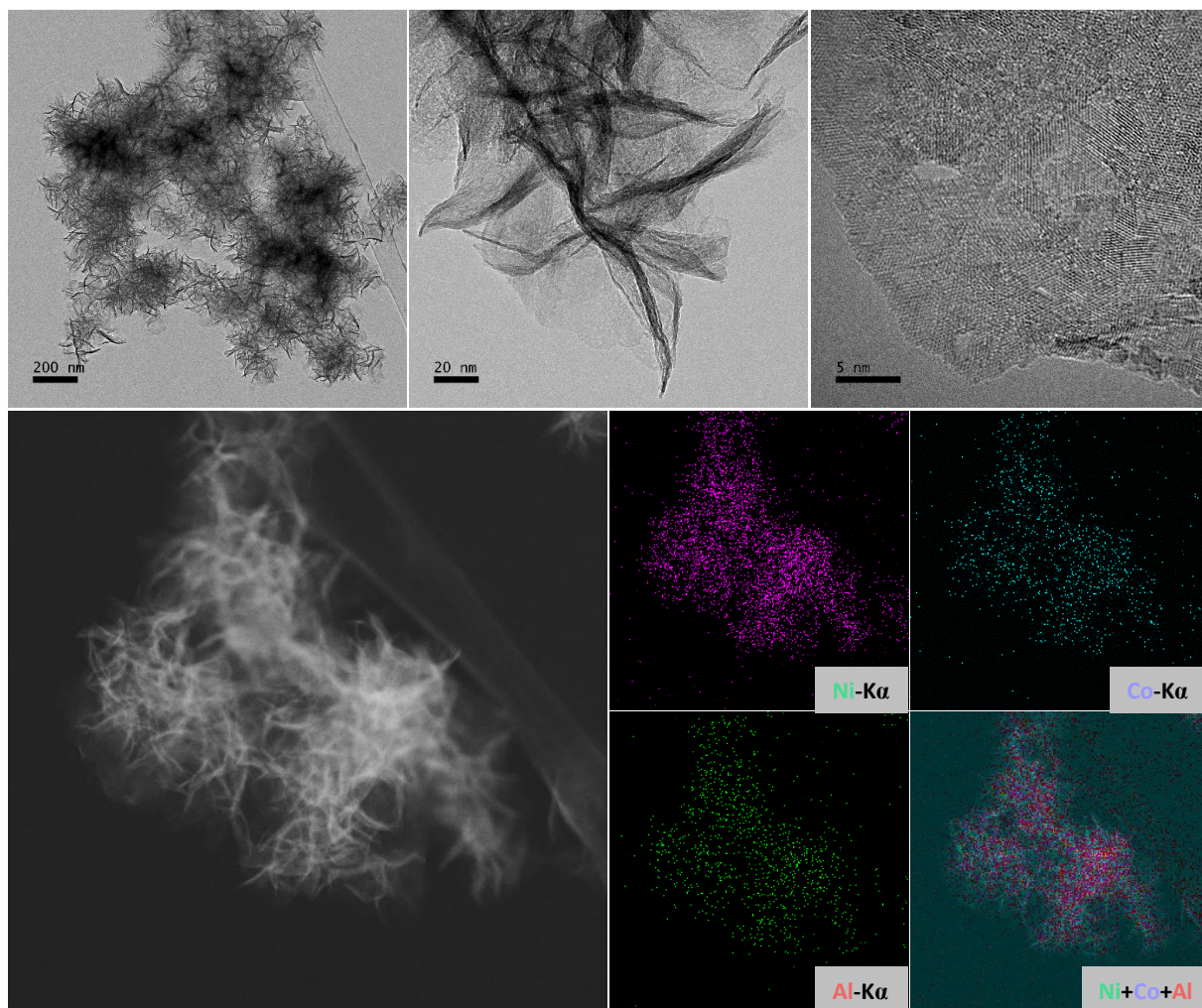


**Fig. S3** TEM images and STEM-EDS mapping images of NCA-LDH sheets.

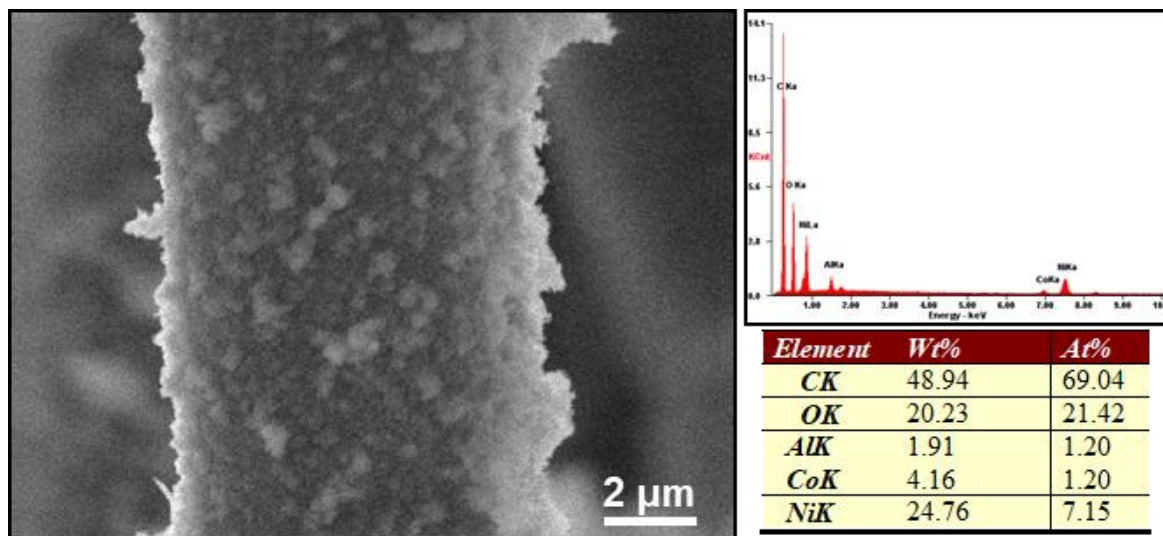


**Fig. S4** SEM image and SEM-EDS spectra of NCA/C electrode.

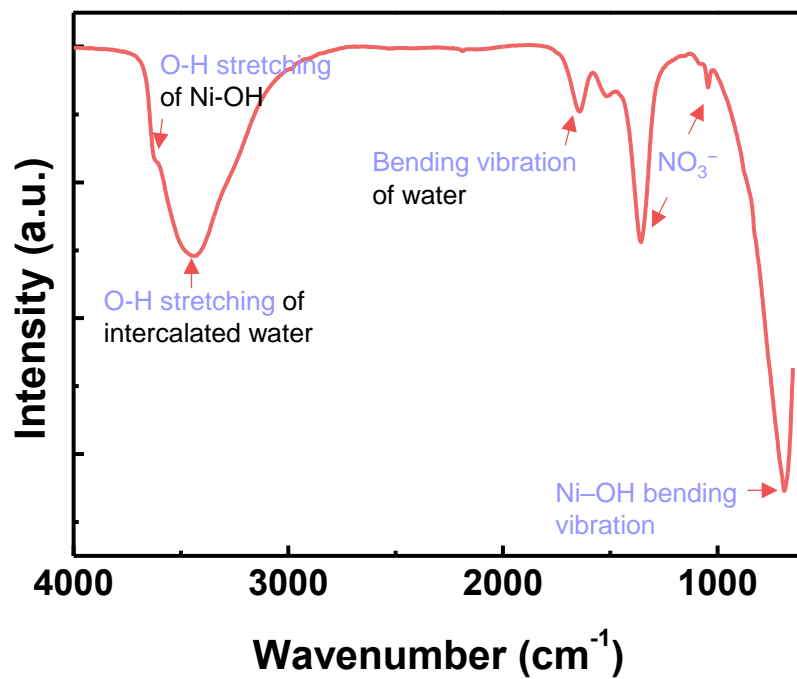


**Fig. S5** FT-IR spectrum of NCA-LDH sheets.

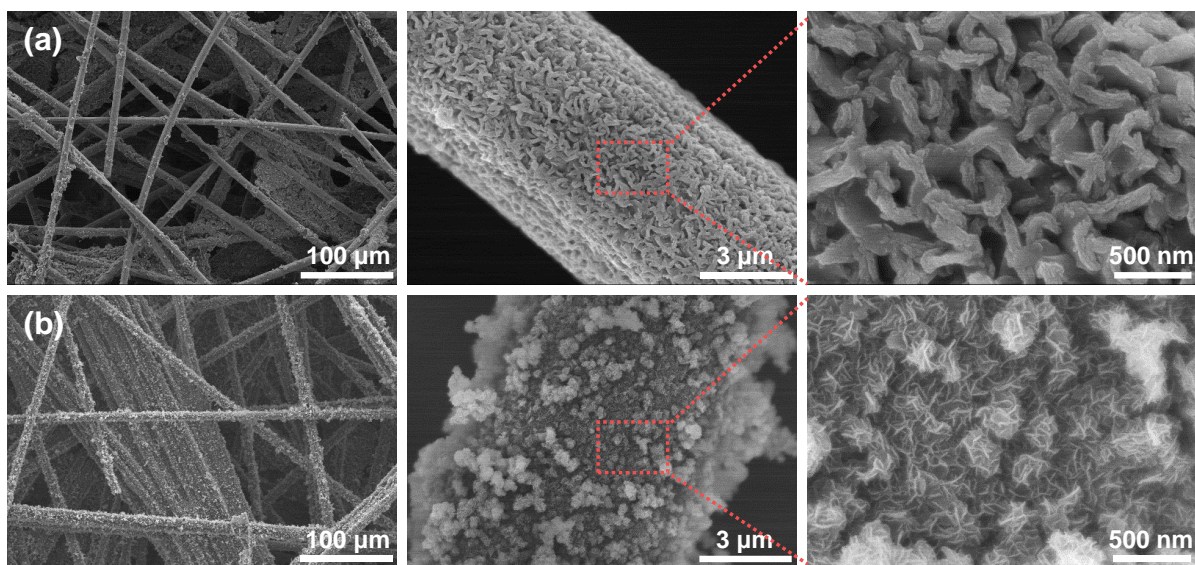


**Fig. S6** SEM images of (a)  $\alpha$ -Ni(OH)<sub>2</sub>/C and (b) NiAl-LDH/C electrodes.

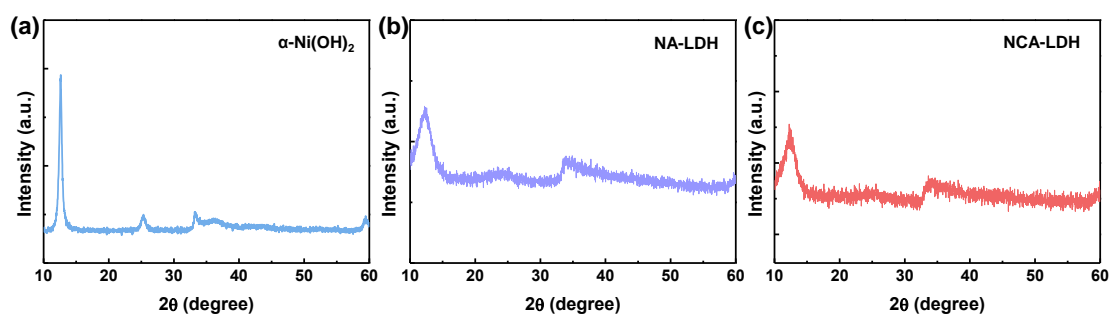


**Fig. S7** Comparative XRD results for (a) the  $\alpha$ -Ni(OH)<sub>2</sub>/C, (b) NiAl-LDH/C, and (c) NCA-LDH/C electrodes.



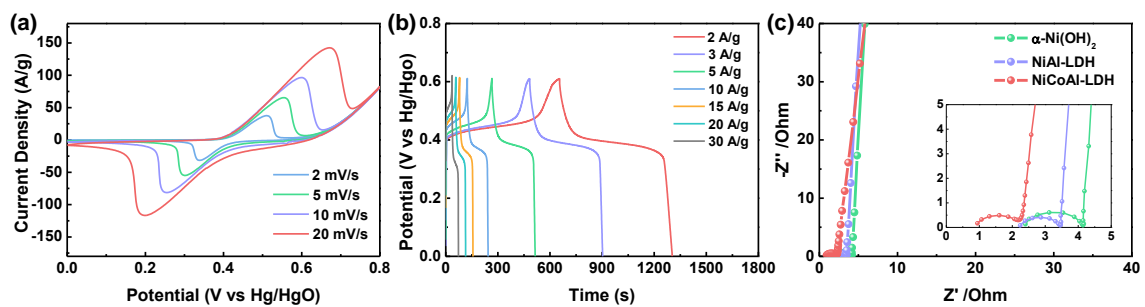


**Fig. S8** Electrochemical results for NCA-LDH/C. (a) CV curves at different current rates. (b) Galvanostatic charge–discharge curves. (c) EIS analysis of NCA-LDH/C electrode.

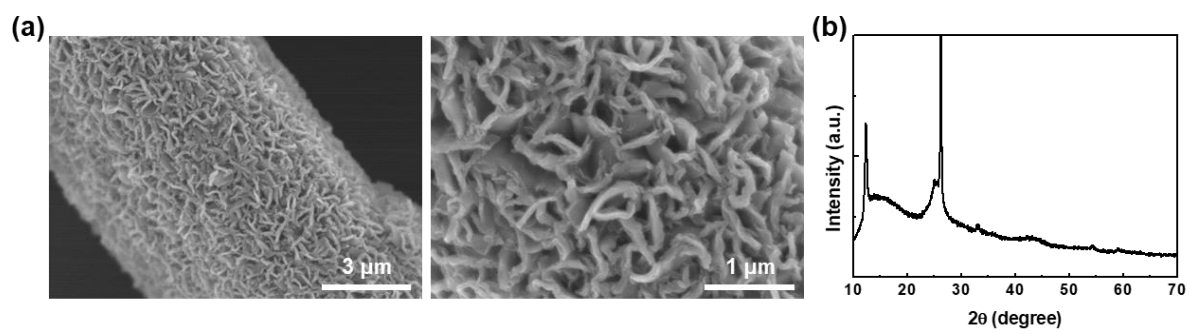


**Fig. S9** (a) SEM images and (b) XRD spectra of NiCo-LDH/C electrode.

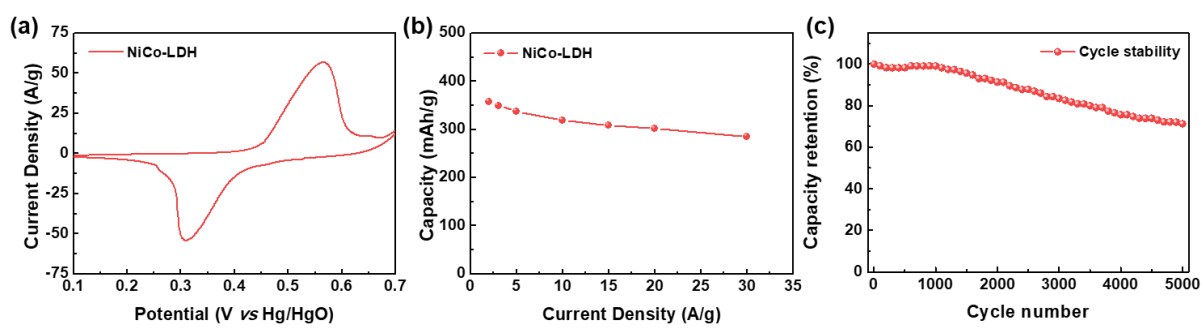


**Fig. S10** (a) CV curve, (b) specific capacity as the current density and (c) cycle stability of NiCo-LDH/C electrode.

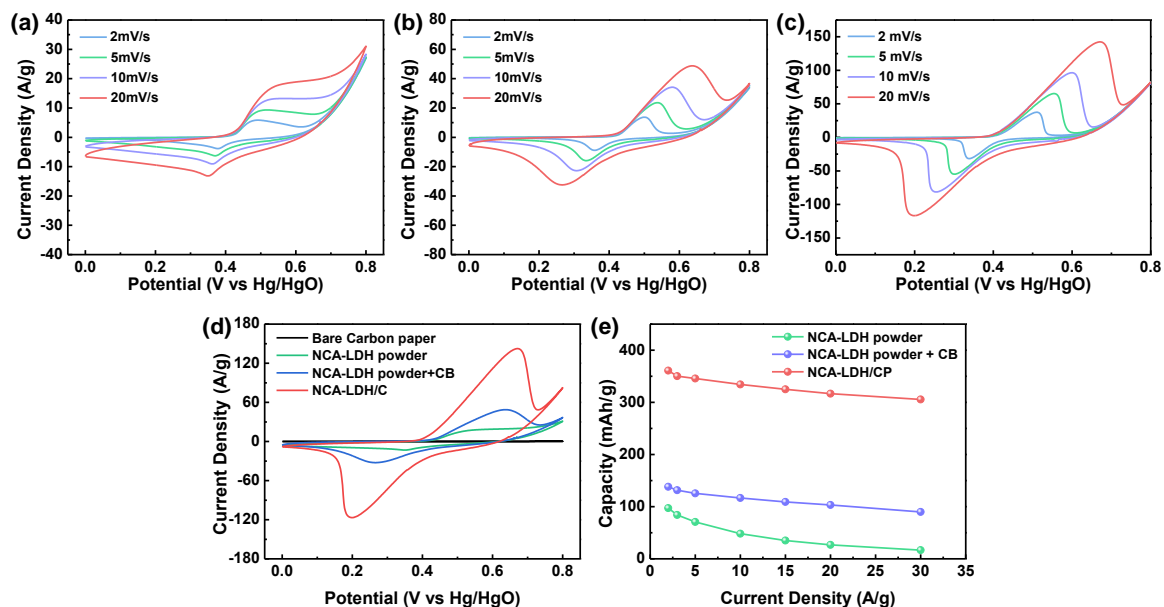


**Fig. S11** Electrochemical results for NCA powder, NCA powder + carbon black (CB), and the NCA-LDH/C electrode. CV curves of (a) NCA powder, (b) NCA powder + CB, and (c) the NCA-LDH/C electrode. (d) Summary of CV curves and (e) Comparative rate capability of NCA powder, NCA powder + carbon black (CB), and the NCA-LDH/C electrode.

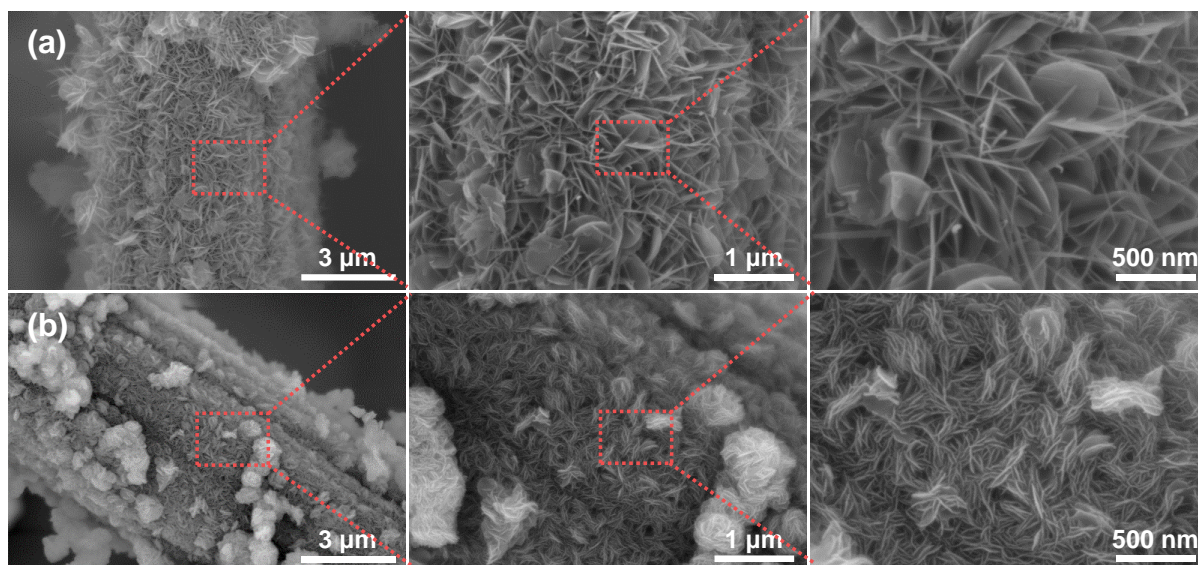


**Fig. S12** SEM images of NCA-LDH/C electrode with different solvent mixtures. (a) DI water: DMF = 9:1. (b) DI water: DMF = 5:5.

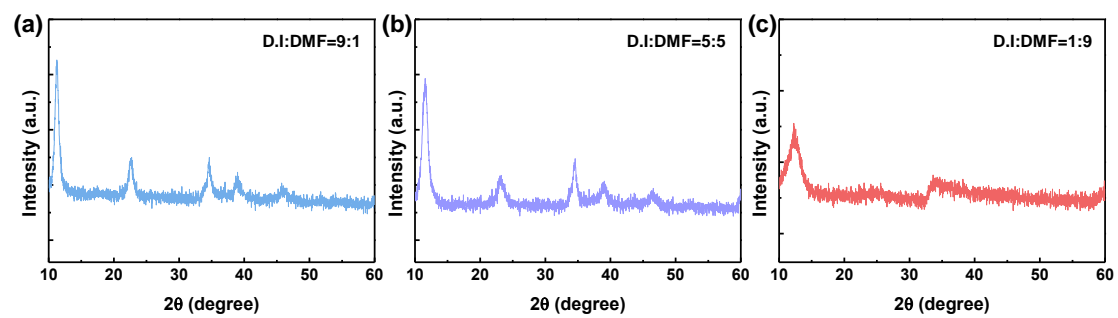


**Fig. S13** Comparative XRD results with different solvent mixtures. (a) DI water: DMF = 9:1. (b) DI water: DMF = 5:5. (c) DI water: DMF = 1:9.

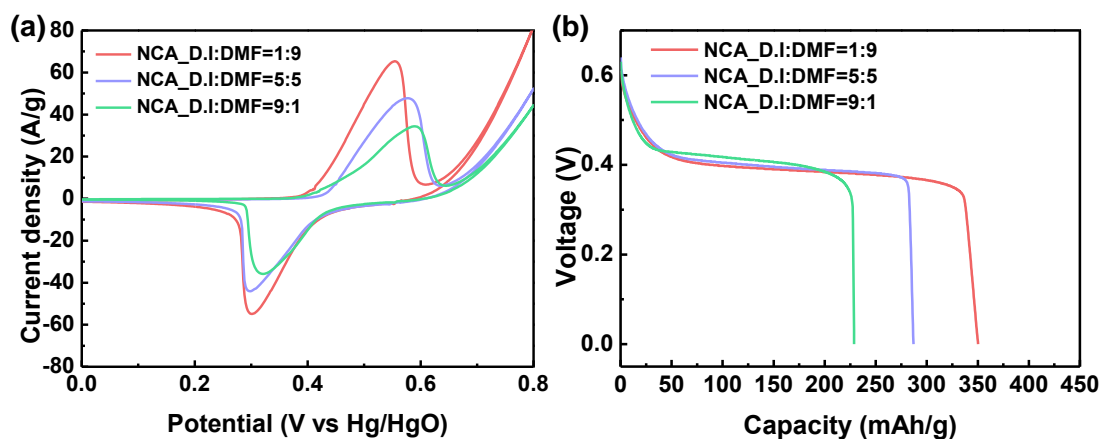


**Fig. S14** Electrochemical results for NCA-LDH/C with different solvent mixtures. (a) Summary of CV curves and (b) Galvanostatic discharge curves with with different solvent mixtures

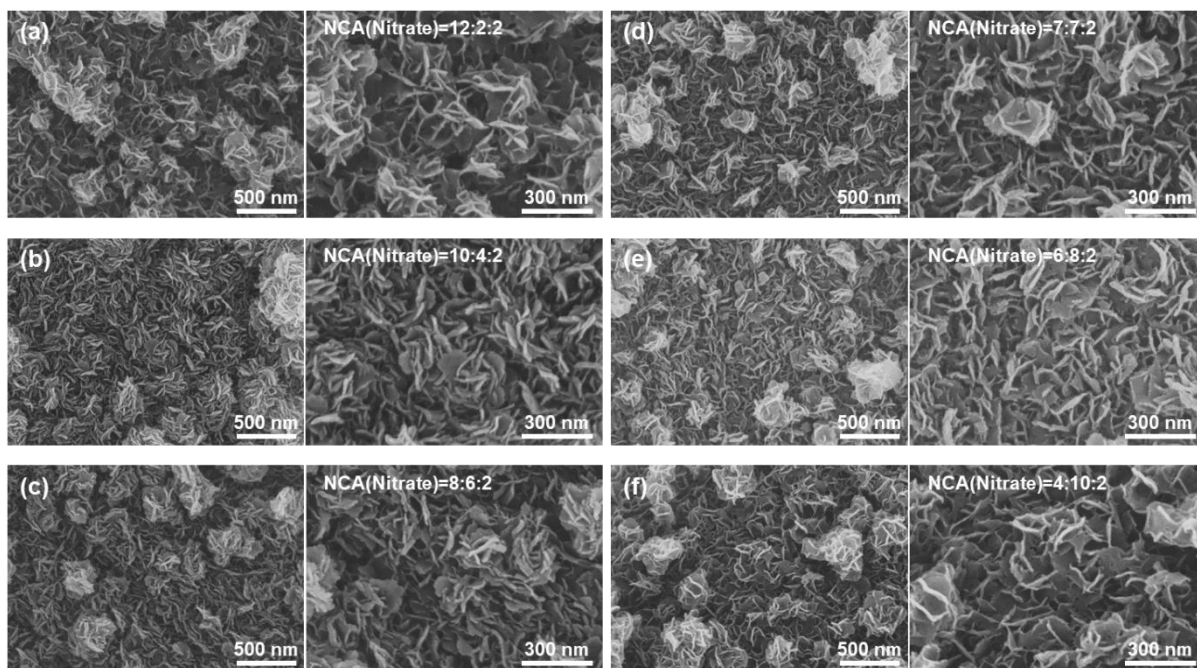


**Fig. S15** SEM images of NCA-LDH/C electrode as the different ratio of Ni, Co, Al atom.



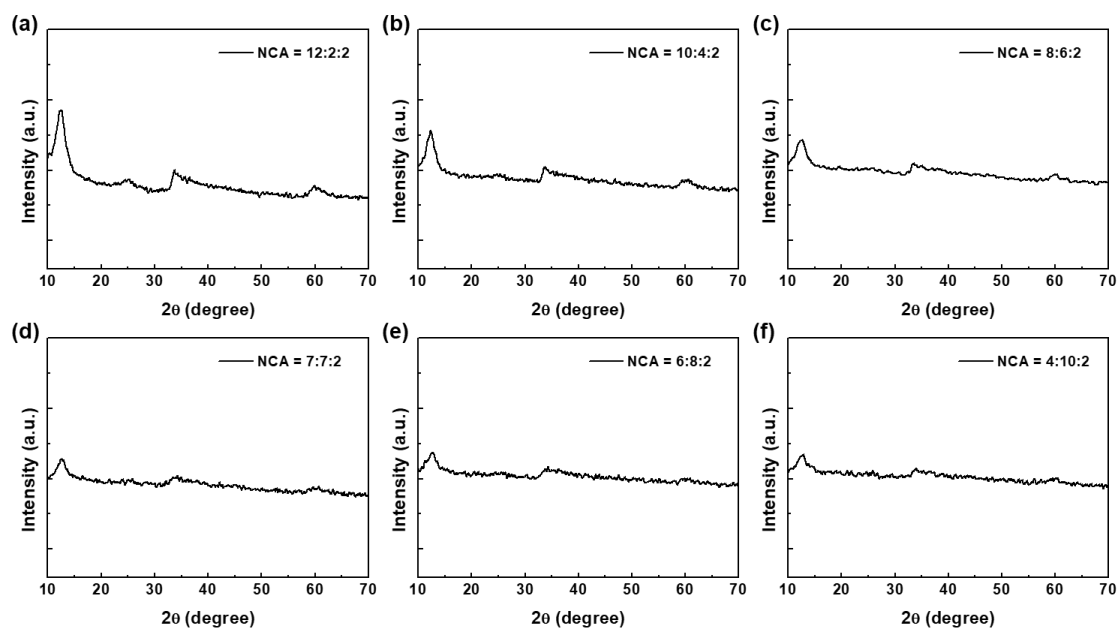


**Fig. S16** XRD spectra of NCA-LDH electrode as the different ratio of Ni, Co, Al atom.

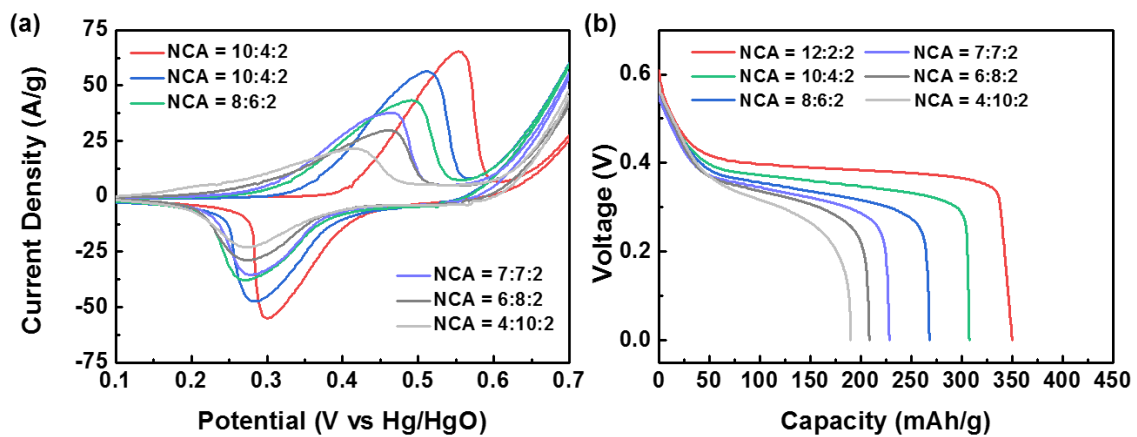


**Fig. S17** (a) CV curve and (b) discharge curve of NCA-LDH/C electrode as the different ratio of Ni, Co, Al atom.

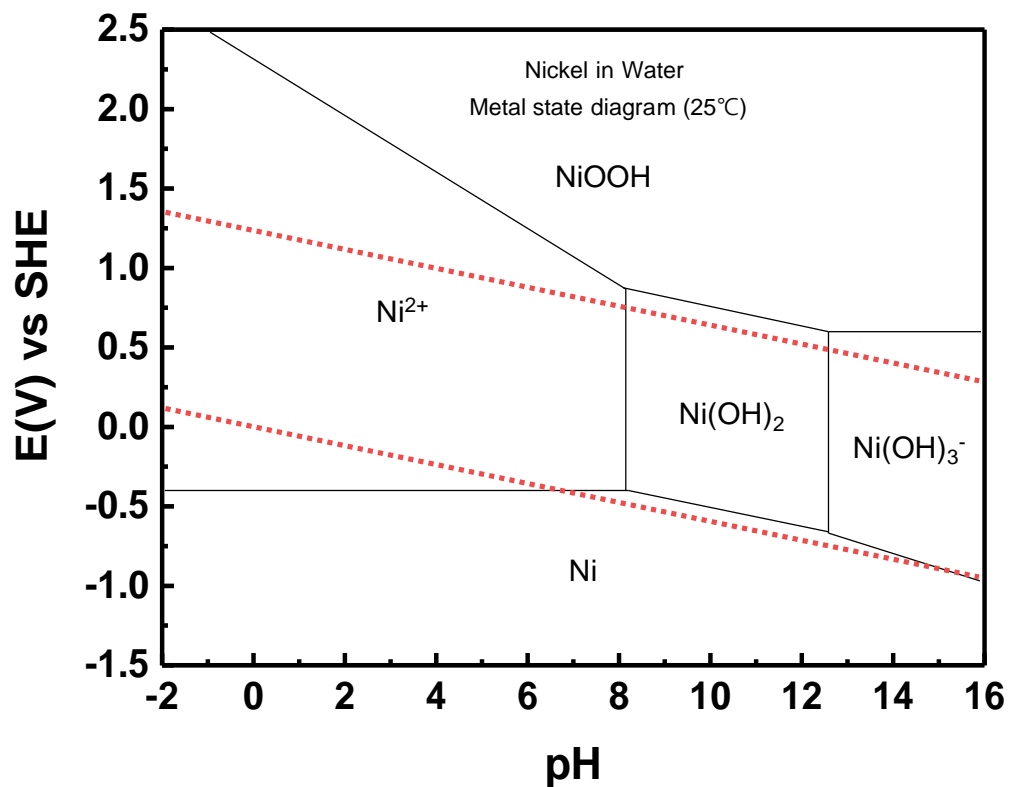


**Fig. S18** Pourbaix diagram of  $\text{Ni}(\text{OH})_2$ , which represents the relationship between the potential and pH.<sup>1</sup> The reduction potential of  $\text{Ni}(\text{OH})_2$  is dependent on the pH value (which corresponds to the concentration of NaOH solution), leading to the variable operating voltage of the Na/Ni battery as the concentration of NaOH.

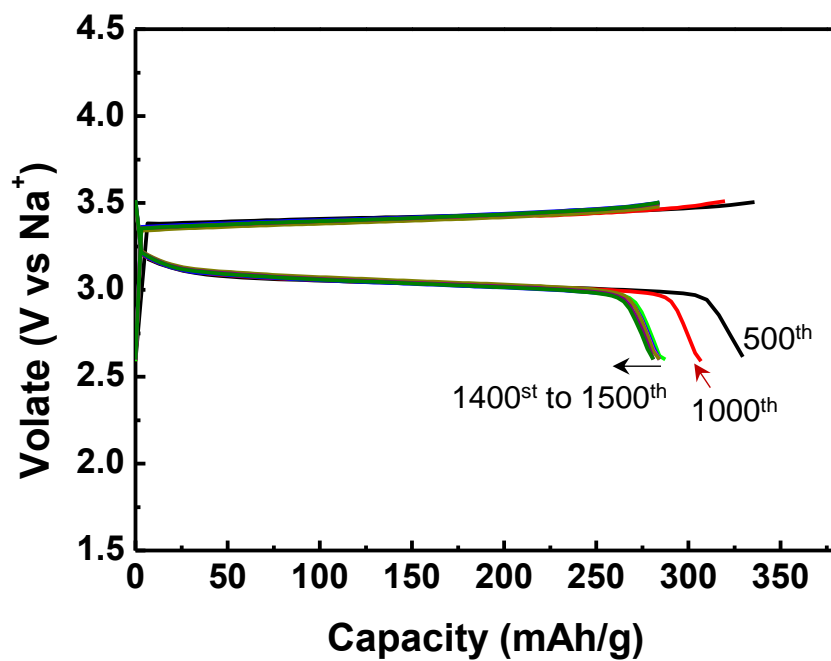


**Fig. S19** Typical charge-discharge curves of Na-Ni battery during 1500 cycles.

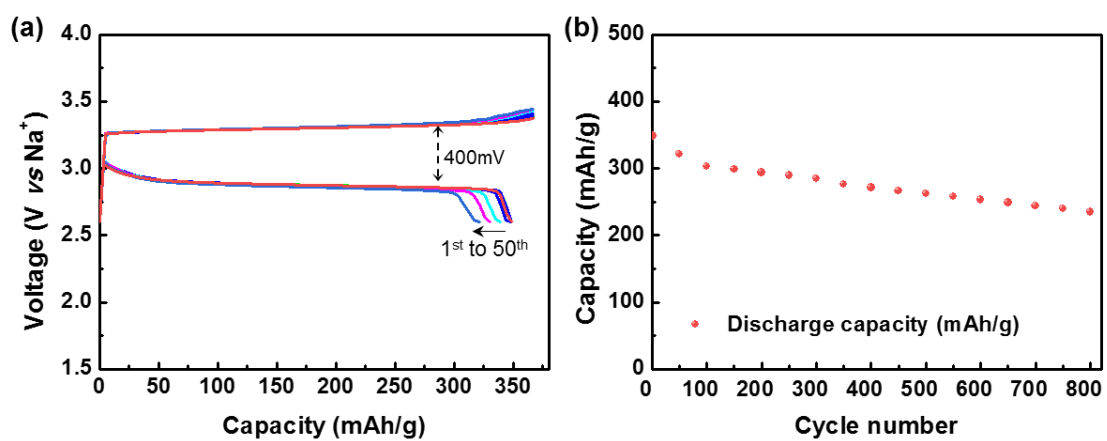


**Fig. S20** (a) Charge-discharge profile and (b) cycle stability of Na-Ni battery in 5M NaOH.

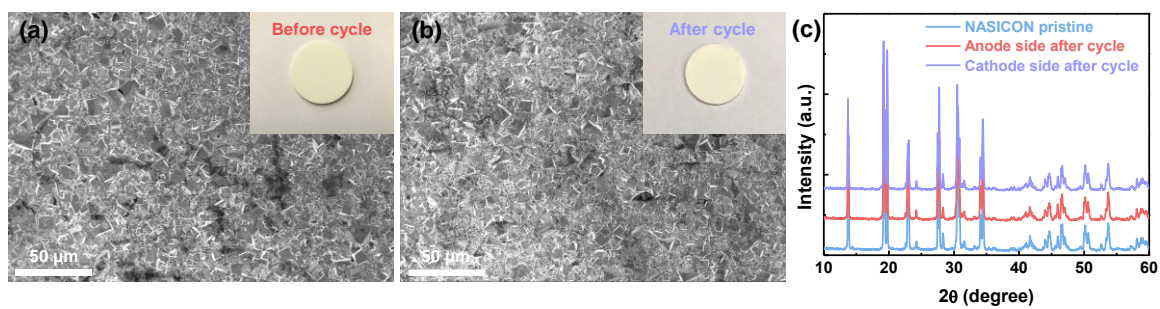


**Fig. S21** Characteristics of NASICON after charge–discharge cycling. (a) SEM images of NASICON (a) before and (b) after cycle test of Na/Ni battery. The inset shows the photo images of NASICON. (c) XRD pattern of NASICON before and after cycle test.

**Table S1.** Comparative results for rechargeable battery systems.

	<i>Anode</i>	<i>Cathode</i>	<i>Voltage (V)</i>	<i>Capacity (mAh g<sup>-1</sup>)</i>	<i>Energy density (Wh kg<sup>-1</sup>)</i>	<i>Ref.</i>
<i>Li-ion</i>	Graphite	LiCoO <sub>2</sub>	3.9	120	468	2
<i>NiMH</i>	Metal hydride	Ni(OH) <sub>2</sub>	1.28	160	205	3
<i>Aqueous Na-ion</i>	Na <sub>0.44</sub> MnO <sub>2</sub>	Carbon	1.1	45	49.5	4
<i>TiO<sub>2</sub>/Ni(OH)<sub>2</sub></i>	TiO <sub>2</sub>	Ni(OH) <sub>2</sub>	1.74	68.7	119.5	5
<i>Fe/Ni</i>	FeOx	β-Ni(OH) <sub>2</sub>	1.04	115	120	6
<i>Zn/Co</i>	Zn	Co <sub>3</sub> O <sub>4</sub>	1.78	135	288	7
<i>Zn/Mn</i>	Zn	MnO <sub>2</sub>	1.44	285	410	8
<i>Na/Ni</i>	Na	NiCoAl- LDH/C	3.1	350	<b>1085</b>	<b>This work</b>

## Supplementary references

- 1 Carmichael, C. Making Economical, Green, High-Energy Nickel-Manganese (NiMn) Batteries, Available online: <http://www.saers.com/recorder/craig/TurquoiseEnergy/BatteryMaking/BatteryMaking.html>
- 2 Pan, H., Shao, Y., Yan, P., Cheng, Y., Han, K. S., Nie, Z., Wang, C., Yang, J., Li, X., Bhattacharya, P., Mueller, K. T., Liu, J. *Nat. Energy* 2016, **1**, 16039.
- 3 Kim, H., Hong, J., Park, K.-Y., Kim, H., Kim, S.-W., Kang, K. *Chem. Rev.* 2014, **114**, 11788.
- 4 Okubo, M., Hosono, E., Kim, J., Enomoto, M., Kojima, N., Kudo, T., Zhou, H., Honma, I. *J. Am. Chem. Soc.* 2007, **129**, 7444-7452.
- 5 Li, B., Cao, H., Shao, J., Zheng, H., Lu, Y., Yin, J., Qu, M. *Chem. Commun.* 2011, **47**, 3159-3161.
- 6 Liu, S., Pan, G. L., Yan, N. F., Gao, X. P. *Energy Environ. Sci.* 2010, **3**, 1732.
- 7 Wang, X.; Wang, F.; Wang, L.; Li, M.; Wang, Y.; Chen, B.; Zhu, Y.; Fu, L.; Zha, L.; Zhang, L.; Wu, Y.; Huang, W. *Adv. Energy Mater.* 2016, **28**, 4904-4911.
- 8 Wang, H., Liang, Y., Gong, M., Li, Y., Chang, W., Mefford, T., Zhou, J., Wang, J., Regier, T., Wei, F., Dai, H. *Nat. Commun.* 2012, **3**, 917.